



Ultrahigh mobility and nonsaturating magnetoresistance in Heusler topological insulators

Chandra Shekhar,^{*} Siham Ouardi, Ajaya K. Nayak, Gerhard H. Fecher, Walter Schnelle, and Claudia Felser[†]
Max Planck Institute for Chemical Physics of Solids, 01187 Dresden, Germany

(Received 21 August 2012; published 19 October 2012)

We report the transport properties of the proposed Heusler topological insulators YPtSb, LaPtBi, and LuPdSb. All compounds show ultrahigh hole mobility with value of 4124, 4275, and 1800 cm² V⁻¹ s⁻¹ for YPtBi, LaPtBi, and LuPdSb, respectively, at 300 K. The temperature dependence of mobility shows strong and weak phonon scattering for LaPtBi and LuPdSb, respectively, while YPtSb shows strong impurity scattering. These ultrahigh values of the mobility are not only due to gaplessness but also to the presence of linear dispersion of the bands close to the Fermi energy, where charge carriers behave like relativistic particles. Furthermore, nonsaturating magnetoresistance (MR) is observed in the temperature range 2–300 K that shows linear behavior at high fields. A tentative relationship between the linear MR and mobility is discussed, which indicates that the mobility controls the linear part of MR.

DOI: [10.1103/PhysRevB.86.155314](https://doi.org/10.1103/PhysRevB.86.155314)

PACS number(s): 73.43.Qt, 73.50.Dn, 75.47.—m, 73.23.—b

I. INTRODUCTION

Topological insulators (TIs) are a class of quantum materials and belong to a new state of matter with topologically protected gapless Dirac fermionic states.^{1,2} These gapless states originate from the inversion of bulk bands. Three-dimensional (3D) TIs contain such surface states, which are promising candidates for the nanoelectronic devices.^{1,3} The performance of these devices can be improved by increasing mobility counts in the system. Over hundreds of TIs have been predicted by various groups.^{4–13} Among them Heusler compounds are promising candidates showing topological properties.^{9–13} The Heusler compounds (TT'M) possess MgAgAs-type face-centered-cubic (space group $F\bar{4}3m$) crystal structure,¹⁴ where T, T', and M atoms occupy Wyckoff position 4b, 4c, and 4a, respectively. Usually, they consist of transition or rare earth metals (T,T') with one main group element (M) in 1:1:1 stoichiometry. Besides the topological property, these materials are well known due to many different intriguing and extraordinary physical properties like the linear dispersion relation of bands along with *zero band gap*^{15–17} and various other properties that have been reported in our review.¹⁸ Therefore, these materials are often called “*compounds with properties on request*”.¹⁹

Generally, gapless compounds show high mobility,²⁰ where no threshold energy is required to conduct carriers from occupied states to empty states. Very recently, the exciting discovery of graphene is another example of high-mobility compounds²¹ due to its linear dispersion of the bands, where charge carriers behave like massless particles. Moreover, the mobility plays a central role for charge transport in a material, which is critically related to the device efficiency. High mobility value reveals high carrier transport, and consequently increases the efficiency of various devices, such as solar cells,²² thermoelectric materials,²³ and transistors.^{24,25} Therefore, mobility is an important factor for low-power and high-speed device applications which have been proposed for TIs. Recently, several studies on bulk transport of TIs have come out and the most familiar examples are Bi₂Se₃ and Bi₂Te₃ that show high mobility.^{26,27} In general, the polycrystalline half Heusler compounds show low mobility and are not categorized in the

TI family.^{28–30} Even though some polycrystalline Heuslers show topological properties, only a small value of mobility of the order of 160 cm² V⁻¹ s⁻¹ has been reported.^{31,32} But these reported compounds are either metallic or narrow-gaped semiconductors. However, the Heusler TIs having zero gap are expected to show high mobility, as the charge carriers behave like massless Dirac fermions. Additionally, their bands exhibit linear dispersion close to the Fermi energy.^{15–17} Furthermore, if the advantages of high mobility are successfully implemented in nanospintronic devices based on TIs, a significant saving of energy will be accomplished. From the above facts, therefore, it is encouraging and worthwhile to search for high-mobility TIs.

II. EXPERIMENTAL DETAILS

Polycrystalline samples of YPtSb, LaPtBi, and LuPdSb were synthesized by arc melting stoichiometric amounts of the constituent elements in a high-purity argon atmosphere. For better homogeneity and crystallinity, the arc-melted ingots were wrapped in Ta foil and then annealed in evacuated quartz tubes at 1073 K for two weeks. Multiple batches of the samples were prepared with antimony or bismuth excess to compensate the weight losses, which is responsible for the variation of carrier concentrations. The composition and structure were checked by energy-dispersive x-ray analysis (EDX) and x-ray diffraction (XRD), respectively. The powder XRD analysis revealed a single phase with MgAgAs-type cubic crystal structure and the lattice parameters of 6.5296, 6.8448, and 6.4263 Å are calculated for YPtSb, LaPtBi, and LuPdSb, respectively, by the least squares method. These values are in good agreement with our previous reported values.^{15,17} The ingots of highly stoichiometric annealed samples were cut into slices with suitable size for further transport measurements. The transport measurements were performed using a quantum design physical property measurement system (PPMS) with the standard low-frequency lock-in technique in the temperature range from 2 to 310 K. Four-probe resistivity and five-probe Hall coefficient measurements were carried out by the conventional ac bridge technique in the Ohmic limit.

III. RESULTS AND DISCUSSION

Temperature dependence of resistivity of a material reflects scattering of charge carriers with phonon and impurities at high and low temperatures, respectively. Figures 1(a) and 2(a) show the magnitude and an overview of the temperature dependence of the electrical resistivity $\rho(T)$, of YPtSb, LaPtBi, and LuPdSb. The observed ρ value of 1.5 m Ω cm for YPtSb and 2.1 m Ω cm for LuPdSb at 300 K are consistent with those for other members of the REPd(Pt)Sb series.^{15,17,33} However, the value of ρ , 37 $\mu\Omega$ cm for LaPtBi, is nearly two order of magnitudes lower in comparison with the value for YPtSb and LuPdSb due to high carrier density, which may be an issue of further discussion. The resistivities of YPtSb and LaPtBi increase with temperature and go through a broad maxima at $T_{\max} = 210$ and 140 K, respectively. Further with the increase of temperature, the resistivities decrease due to activation of charge carriers. This is the typical behavior of semimetal or gapless compounds and is commonly seen in such types of compounds that do not show large activation energy, like semiconductors.^{15,31} Although no such broad transition is observed in LuPdSb up to 310 K, the resistivity saturates at higher temperatures indicating the transition may exist beyond 310 K. The resistivity below T_{\max} is reminiscent of the behavior of highly doped semiconductors, where some donor or acceptor levels are formed. In the the

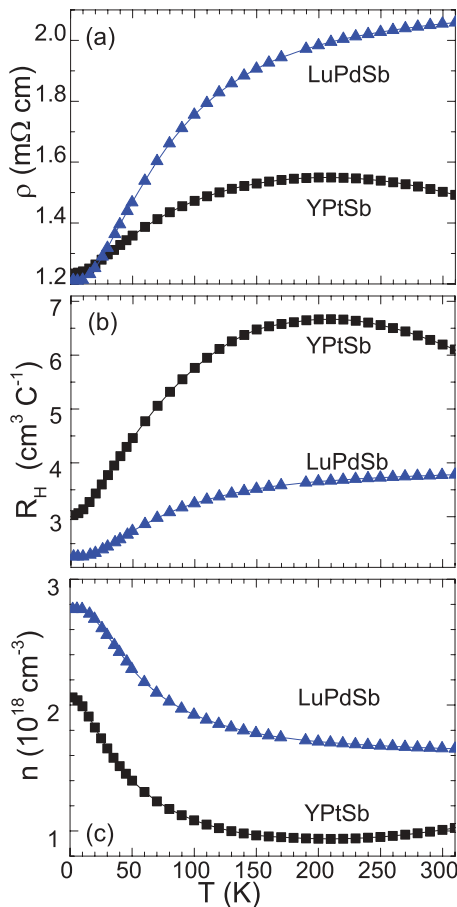


FIG. 1. (Color online) Temperature dependence of (a) resistivity, (b) Hall coefficients, and (c) carrier densities of YPtSb and LuPdSb.

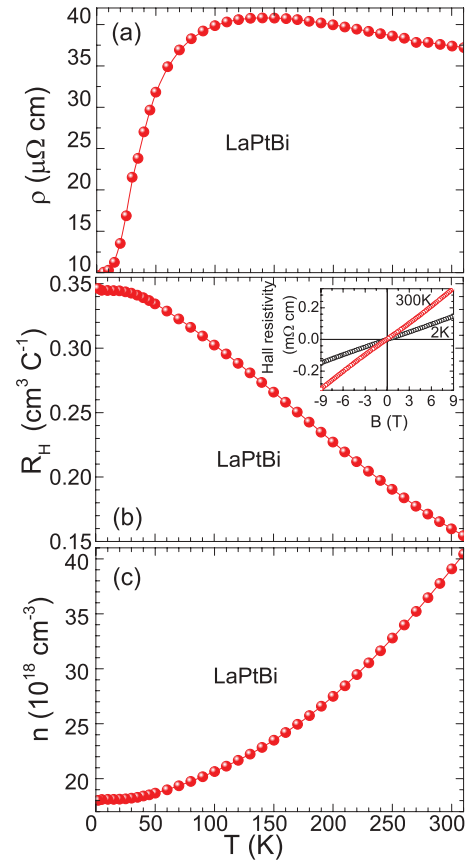


FIG. 2. (Color online) Temperature dependence of (a) resistivity, (b) Hall coefficient, and (c) carrier density of LaPtBi. The inset shows the linear behavior of the Hall resistivity of LaPtBi with field. Other compounds also show a similar linear behavior.

present case, this may be due to atomic disorders or little variation in the stoichiometry which governs the conduction at low temperature. These defects commonly arise when materials are synthesized by arc melting.^{17,31} This effect can also be seen in YPtSb where the resistivity behavior differs at low temperatures in the earlier report.¹⁷ However, the magnitude and temperature dependency of resistivity at higher temperature are similar. On the other hand, if the vacancies present in the compound are in the form of a sublattice then a narrow gap appears at the Fermi level resulting in a negative temperature dependence of resistivity at low temperature.³⁴ But this behavior is ruled out in the present case because they neither have a gap nor show negative temperature dependence of resistivity at low temperature.

The experimental investigation of the Hall effect in the semiconductor is instrumental in deriving information on the most important kinetic parameters, such as charge carrier concentration and mobility. Therefore, we performed the Hall-effect measurements in a temperature sweep as well as field sweep modes of our well-characterized polycrystalline samples. A linear Hall resistance is found in the field sweep measurements in the temperatures range of 2–310 K with fields up to 9 T for all compounds as shown in the inset of Fig. 2(b). This linear Hall resistivity indicates the involvement of only one type of charge carrier in transport properties, whereas nonlinear Hall resistivity shows the involvement of

more than one type of carrier.³⁵ Thus, the single-carrier band model will be applied for further calculations. All compounds show positive Hall coefficient $R_H(T)$ [see Figs. 1(b) and 2(b)] throughout the temperatures range from 2–310 K, suggesting that holes are the predominant charge carriers. The overall behavior of $R_H(T)$ coincides with that of the resistivity in YPtSb and LuPdSb. However, $R_H(T)$ of LaPtBi decreases linearly with increasing temperature in contrast to the increasing behavior of the resistivity at low temperature. The values of $R_H(T)$ for YPtSb, LaPtBi, and LuPdSb are 6.2, 0.16, and 3.8 $\text{cm}^3 \text{C}^{-1}$ at 300 K, respectively. The larger values of $R_H(T)$ indicate that these materials belong to the category of low-charge-carrier semimetals or gapless compounds.^{15,17} The charge carrier density is estimated assuming a one-carrier model and its temperature dependency are shown in Figs. 1(c) and 2(c). The estimated values are 2.0×10^{18} , 1.9×10^{19} , and $2.8 \times 10^{18} \text{ cm}^{-3}$ at 2 K and 1.0×10^{18} , 3.9×10^{19} , and $1.7 \times 10^{18} \text{ cm}^{-3}$ at 300 K for YPtSb, LaPtBi, and LuPdSb, respectively. Here, we can say that excess of the bismuth is responsible for higher carrier density of the LaPtBi which restricts material into a low value of resistivity. It can be seen that the carriers densities of YPtSb and LuPdSb decrease as temperature increases showing metal-like behavior, whereas LaPtBi shows increasing behavior with temperature. Since these compounds show zero band gap,^{15,17} any change of carriers density implies a big difference in resistivity. Therefore, these compounds show a different temperature dependence of the resistivity and carrier density. The carrier density data at 300 K are consistent with their resistivity, which means low-carrier-density compounds have high resistive values and vice versa. The Hall mobility, μ_H of YPtSb, LaPtBi, and LuPdSb are calculated by using the formula $\mu_H(T) = R_H(T)/\rho(T)$, which is shown in Fig. 3. The temperature-dependent value of the mobility ranges from 2457 to 4124 $\text{cm}^2 \text{V}^{-1} \text{s}^{-1}$ for YPtSb and 35 900 to 4275 $\text{cm}^2 \text{V}^{-1} \text{s}^{-1}$ for LaPtBi between 2–300 K. In contrast, LuPdSb shows negligible temperature dependence of mobility with a constant value of 1800 $\text{cm}^2 \text{V}^{-1} \text{s}^{-1}$. All these mentioned values are ultrahigh in comparison with recent reports of other similar compounds,^{31,32} where the maximum reported value of mobility is 160 $\text{cm}^2 \text{V}^{-1} \text{s}^{-1}$ at 300 K. Such a high value of mobility has not been observed in any of the polycrystalline Heusler compounds, which are found to be comparable to that of other series of single-crystal TIs.^{26,27} The temperature-dependent mobility mainly arises due to two different types of scattering mechanisms of charge carriers. First, the ionized impurity scattering gives a mobility temperature dependence with a positive power law. Second, lattice vibration scattering gives a mobility temperature dependence with a negative power law. Hence, the temperature-dependent mobility of YPtSb is a mixed example of both cases: first mobility increases with $T^{0.23}$ behavior up to 150 K due to ionized impurity scattering and afterward it decreases due to lattice scattering. For LaPtBi, mobility continuously decreases with T and follows a $T^{-0.62}$ behavior, reflecting the dominant role of lattice scattering over the temperature range 2–300 K. The mobility of LuPdSb shows a typical behavior with temperature and has a negligible temperature variation of $T^{-0.0075}$ in comparison with YPtSb and LaPtBi. In one band model, the mobility is inversely proportional to the scattering rate and effective mass. And

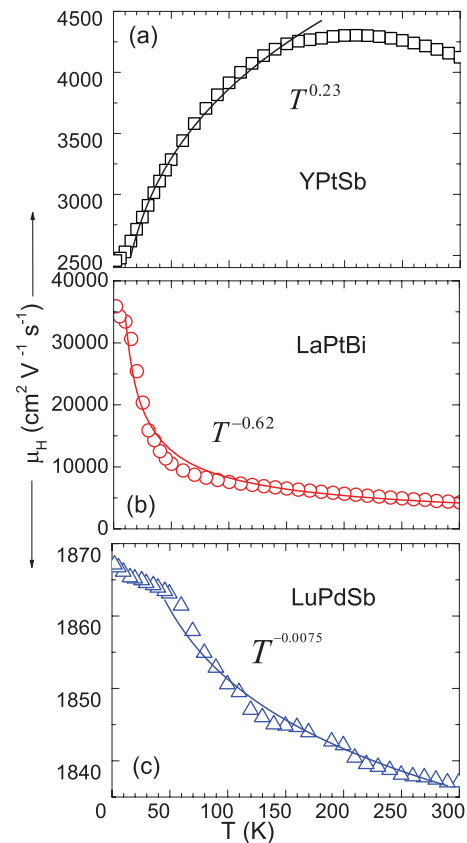


FIG. 3. (Color online) Temperature dependence of Hall mobility of (a) YPtSb, (b) LaPtBi, and (c) LuPdSb. The lines indicate their power variation with temperature.

on the other hand, the compounds with small energy gaps at direct band edges have high values of carrier mobility. Therefore, a high mobility can be realized in small-band-gap and light-effective-mass compounds. Taking into account the material properties, therefore, the observed high values of mobility mainly originate from two possible routes: (i) due to zero band gap^{15,17,20} where no threshold energy is required to conduct carriers. (ii) due to the linear dispersion of bands in which the charge carriers possess very low effective mass resulting high mobility.²¹ These Heusler compounds have both these properties and hence show high mobility. The high mobility of TIs are important, not only as a physical phenomena but also for further device applications such as image magnetic monopoles, neutral Majorana fermions, and giant magneto-optical effects.

For technological applications, the magnetoresistance (MR) is important for particular interest. The MR is defined as the changes in resistivity with fields, as $\text{MR}(B) = \rho(B)/\rho(0) - 1$, where B is the applied magnetic field. The field dependence MR of YPtSb and LaPtBi at selected temperatures is shown in Fig. 4 and the MR of LuPdSb is shown in Figs. 5(a) and 5(b). The following are the remarkable features of the observed MR: The overall patterns are nonsaturating and positive that show systematic variations with temperature and field. For example, we fit the MR of YPtSb at 2 K as shown in Fig. 5(c). The best fitting is found with the combination of linear and quadratic field dependence

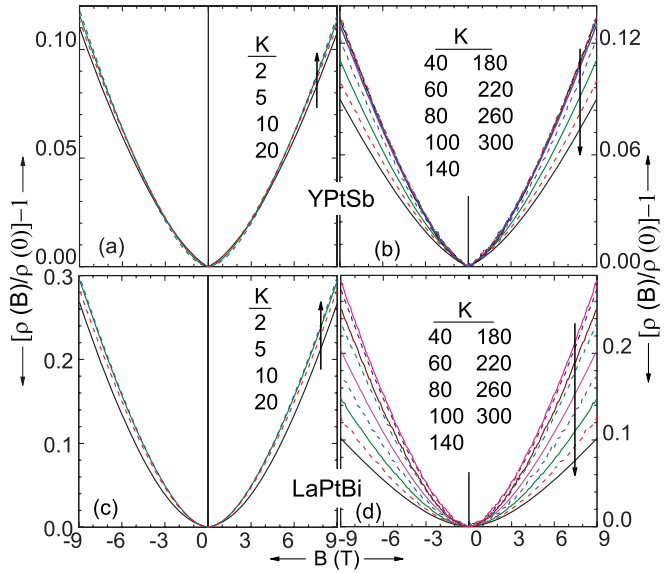


FIG. 4. (Color online) Field dependence of MR of (a) YPtSb at $T \leq 20$ K, (b) YPtSb at $T \geq 40$ K, (c) LaPtBi at $T \leq 20$ K, and (d) LaPtBi at $T \geq 40$ K. All MR show similar field dependency.

of the MR and may be written in form of a quadratic equation: $MR = a|B| + (b/2)B^2$. However, the regular metals exhibit only a B^2 dependence of MR which saturates at high fields. For temperatures above 20 K, the MR of YPtSb, LaPtBi, and LuPdSb also show similar behavior which can be seen in Figs. 4(b), 4(d), and 5(b). In order to get a broad view of the turning point of MR, the first-order derivative of MR of LaPtBi with field at 20 K is plotted in Fig. 5(d). In this figure, two lines are drawn from 0 and 9 T fields which intersect each other at the field of 2.4 T. This value of field indicates a turning point between parabolic and linear MR that is nearly constant with

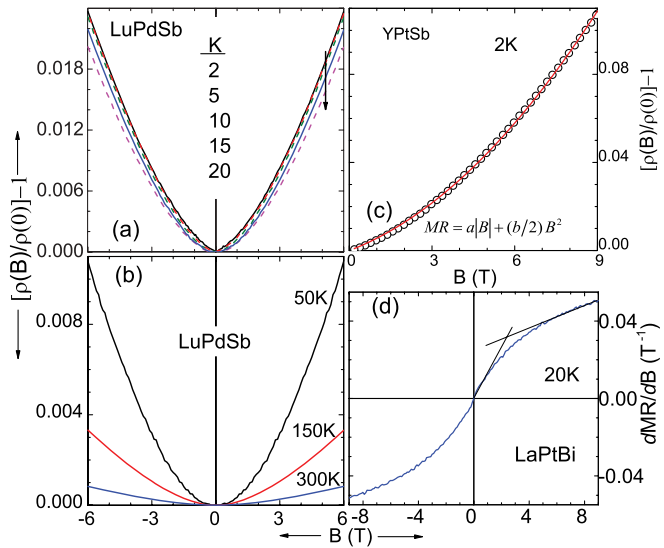


FIG. 5. (Color online) Field dependence of MR of (a) LuPdSb at $T \leq 20$ K, (b) LuPdSb at $T \geq 50$ K. (c) For an example, the observed MR of YPtSb at 2 K (open circles) and fit (red line) with the quadratic equation $MR = a|B| + (b/2)B^2$. (d) First derivative of MR of LaPtBi with field at 20 K, the intersection of lines indicates a turning point between parabolic and linear MR.

temperature, which means linear and parabolic contributions are independent of temperature, which is unlikely in this class of materials. For temperatures below 20 K, the MR increases slowly for YPtSb and LaPtBi. From the above observations it is very much clear that the MR originates from the contribution of both linear and parabolic terms. The parabolic term is well known and comes from the Lorentz force, while the origin of the linear MR is intriguing. It has been reported that some of the nonmagnetic compounds show nonsaturating linear MR including TIs,^{15,36,37} where both quantum³⁶ and classical^{37,38} theories have been applied. However, there is no direct evidence of quantum MR, properties like linear dispersion of bands,^{15,17} high mobility, and temperature-independent MR at low temperatures are favorable conditions to suggest the presence of quantum MR in the present compounds. On the other hand, a classical model has been proposed by Parish *et al.* where linear MR is expected to be governed by mobility.³⁸

To examine the role of mobility on the observed MR, we calculated the slope of the linear part of the MR and the mobility at different temperatures. The slope, dMR/dB and carrier mobility are plotted on left and right axes, respectively, as a function of inverse temperature, as shown in Fig. 6. The part of the data connected by the dotted line in Fig. 6(c) shows a $T^{-0.0075}$ dependency for temperature above 50 K. However, it has already been discussed and shown in Fig. 3(c) that the mobility also shows a best fit to the same power of $T^{-0.0075}$ for temperatures above 50 K. Similarly, other power dependencies can also be found for YPtSb and LaPtBi which are same as for

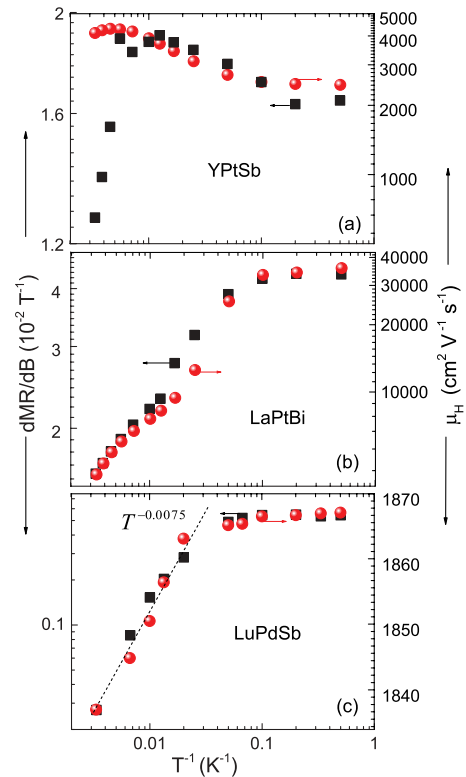


FIG. 6. (Color online) Linear part of the slope of the MR; that is, dMR/dB (filled squares) on left scale and carrier mobility (filled spheres) on right scale as a function of inverse temperature for (a) YPtSb, (b) LaPtBi, and (c) LuPdSb. The dotted line through the data represents the power dependence.

the mobility of Figs. 3(a) and 3(b), respectively. It is pointed out that dMR/dB and μ_H show identical power relations. Therefore, we infer that the MR and μ_H follow qualitatively a tentative relation $MR(T) = \mu_H(T)B$, which has been reported in recent works.^{15,39} The classical theory suggests that fluctuation of mobility or mobility itself is responsible for the linear MR.^{15,38} Therefore, we can finally conclude that the linear part of MR of these class of materials is controlled by mobility. From Fig. 6(a), it is also noticeable that the similarity between the slope of MR and the mobility of YPtSb deviate from each other above 150 K, which can be understood in terms of a change in the scattering mechanism in the mobility with temperature.³⁹ The observed MR behavior of presently investigated compounds are similar to the MR of nanosheets of the Bi₂Te₃ topological insulator,⁴⁰ where the origin of the quantum MR has been claimed. Therefore, the properties like gaplessness, linear dispersion of bands, ultrahigh mobility, and low charge carriers point towards the presence of quantum MR in presently investigated compounds.

IV. CONCLUSIONS

In conclusion, we have synthesized the proposed topological insulators YPtSb, LaPtBi, and LuPdSb, which show ultrahigh mobility. These high values of mobility originate from the combined effect of both linear dispersion of bands as well as the gapless character of the compounds. The observed ultrahigh mobility is an important factor for three-dimensional topological insulators for the proposed used in nanoelectronic devices. All compounds show nonsaturating magnetoresistance, most likely controlled by their mobility. The similarity between the slope of the linear part of magnetoresistance and the mobility is lost when the scattering mechanism of mobility changes with temperature. This is another issue for further discussion.

ACKNOWLEDGMENTS

The financial support by the DfG (P 2.3-A in FOR 1464 ASPIMATT) is gratefully acknowledged.

*shekhar@cpfs.mpg.de

†felser@cpfs.mpg.de

¹M. König, S. Wiedmann, C. Brüne, A. Roth, H. Buhmann, L. W. Molenkamp, X.-L. Qi, and S.-C. Zhang, *Science* **318**, 766 (2007).

²H. Zhang, C.-X. Liu, X.-L. Qi, X. Dai, Z. Fang, and S.-C. Zhang, *Nat. Phys.* **5**, 438 (2009).

³M. Veldhorst, C. G. Molenaar, X. L. Wang, H. Hilgenkamp, and A. Brinkman, *Appl. Phys. Lett.* **100**, 072602 (2012).

⁴Z. Xiao, Z. Haijun, W. Jing, F. Claudia, and Z. Shou-Cheng, *Science* **335**, 1464 (2012).

⁵B. Yan, L. Müchler, X. L. Qi, S. C. Zhang, and C. Felser, *Phys. Rev. B* **85**, 165125 (2012).

⁶H.-J. Zhang, S. Chadov, L. Müchler, B. Yan, X.-L. Qi, J. Kübler, S.-C. Zhang, and C. Felser, *Phys. Rev. Lett.* **106**, 156402 (2011).

⁷W. Feng, D. Xiao, J. Ding, and Y. Yao, *Phys. Rev. Lett.* **106**, 016402 (2011).

⁸M. Dzero, K. Sun, V. Galitski, and P. Coleman, *Phys. Rev. Lett.* **104**, 106408 (2010).

⁹S. Chadov, X. Qi, J. Kübler, G. H. Fecher, C. Felser, and S.-C. Zhang, *Nat. Mater.* **9**, 541 (2010).

¹⁰H. Lin, L. A. Wray, Y. Xia, S. Xu, S. Jia, R. J. Cava, A. Bansil, and M. Z. Hasan, *Nat. Mater.* **9**, 546 (2010).

¹¹D. Xiao, Y. Yao, W. Feng, J. Wen, W. Zhu, X.-Q. Chen, G. M. Stocks, and Z. Zhang, *Phys. Rev. Lett.* **105**, 096404 (2010).

¹²X. M. Zhang, W. H. Wang, E. K. Liu, G. D. Liu, Z. Y. Liu, and G. H. Wu, *Appl. Phys. Lett.* **99**, 071901 (2011).

¹³C. Liu, Y. Lee, T. Kondo, E. D. Mun, M. Caudle, B. N. Harmon, S. L. Bud'ko, P. C. Canfield, and A. Kaminski, *Phys. Rev. B* **83**, 205133 (2011).

¹⁴W. Jeitschko, *Metall. Mater. Trans. B* **1**, 3159 (1970).

¹⁵C. Shekhar, S. Ouardi, G. H. Fecher, A. K. Nayak, C. Felser, and E. Ikenaga, *Appl. Phys. Lett.* **100**, 252109 (2012).

¹⁶S. Ouardi, C. Shekhar, G. H. Fecher, X. Kozina, G. Stryganyuk, C. Felser, S. Ueda, and K. Kobayashi, *Appl. Phys. Lett.* **98**, 211901 (2011).

¹⁷S. Ouardi, G. H. Fecher, C. Felser, J. Hamrle, K. Postava, and J. Pistora, *Appl. Phys. Lett.* **99**, 211904 (2011).

¹⁸T. Graf, C. Felser, and S. Parkin, *Prog. Solid State Chem.* **39**, 1 (2011).

¹⁹J. Pierre, R. Skolozdra, J. Tobola, C. Hordequin, M. A. Kouacou, I. Karla, R. Currat, and E. Lelievre-Berna, *J. Alloys Compd.* **262–263**, 101 (1997).

²⁰T. Thio, S. A. Solin, J. W. Bennett, D. R. Hines, M. Kawano, N. Oda, and M. Sano, *Phys. Rev. B* **57**, 12239 (1998).

²¹J.-H. Chen, C. Jang, S. Xiao, M. Ishigami, and M. S. Fuhrer, *Nat. Nanotechnol.* **3**, 206 (2008).

²²M. Park, C. B. Doo, J. W. Yu, M. S. Chun, and S.-H. Han, *J. Ind. Eng. Chem.* **14**, 382 (2008).

²³V. Kutasov, L. Lukyanova, P. Konstantinov, and G. Alekseeva, *Phys. Solid State* **39**, 419 (1997).

²⁴A. T. M. G. Sarwar, M. R. Siddiqui, M. M. Satter, and A. Haque, *IEEE Trans. Electron Devices* **59**, 1653 (2012).

²⁵K. Takei, M. Madsen, H. Fang, R. Kapadia, S. Chuang, H. S. Kim, C.-H. Liu, E. Plis, J. Nah, S. Krishna, Y.-L. Chueh, J. Guo, and A. Javey, *Nano Lett.* **12**, 2060 (2012).

²⁶N. P. Butch, K. Kirshenbaum, P. Syers, A. B. Sushkov, G. S. Jenkins, H. D. Drew, and J. Paglione, *Phys. Rev. B* **81**, 241301 (2010).

²⁷S. Jia, H. Ji, E. Climent-Pascual, M. K. Fuccillo, M. E. Charles, J. Xiong, N. P. Ong, and R. J. Cava, *Phys. Rev. B* **84**, 235206 (2011).

²⁸F. G. Aliev, *Physica B* **171**, 199 (1991).

²⁹K. Yoshisato, O. T. Yuki, and K. Takuji, *Appl. Phys. Lett.* **92**, 012105 (2008).

³⁰K. Kenta, K. Ken, M. Hiroaki, and Y. Shinsuke, *J. Appl. Phys.* **104**, 013714 (2008).

³¹K. Gofryk, D. Kaczorowski, T. Plackowski, A. Leithe-Jasper, and Y. Grin, *Phys. Rev. B* **84**, 035208 (2011).

³²K. Gofryk, D. Kaczorowski, T. Plackowski, J. Mucha, A. Leithe-Jasper, W. Schnelle, and Y. Grin, *Phys. Rev. B* **75**, 224426 (2007).

- ³³K. Mastronardi, D. Young, C.-C. Wang, P. Khalifah, R. J. Cava, and A. P. Ramirez, *Appl. Phys. Lett.* **74**, 1415 (1999).
- ³⁴F. G. Aliev, N. B. Brandt, V. V. Moshchalkov, V. V. Kozyrkov, R. V. Skolozdra, and A. I. Belogorokhov, *Z. Phys. B* **75**, 167 (1989).
- ³⁵Z. Ren, A. A. Taskin, S. Sasaki, K. Segawa, and Y. Ando, *Phys. Rev. B* **82**, 241306 (2010).
- ³⁶A. A. Abrikosov, *Phys. Rev. B* **58**, 2788 (1998).
- ³⁷M. Lee, T. F. Rosenbaum, M.-L. Saboungi, and H. S. Schnyders, *Phys. Rev. Lett.* **88**, 066602 (2002).
- ³⁸M. M. Parish and P. B. Littlewood, *Nature (London)* **426**, 162 (2003).
- ³⁹H. G. Johnson, S. P. Bennett, R. Barua, L. H. Lewis, and D. Heiman, *Phys. Rev. B* **82**, 085202 (2010).
- ⁴⁰X. Wang, Y. Du, S. Dou, and C. Zhang, *Phys. Rev. Lett.* **108**, 266806 (2012).